Influence of electronic parameters on the electric-field gradients induced by H at the probe atom ^{111}In/^{111}Cd in Si

H. Skudlik, M. Deicher, R. Keller, R. Magerle, W. Pfeiffer, D. Steiner, and E. Recknagel
Fakultät für Physik, Universität Konstanz, D-7750 Konstanz, Federal Republic of Germany

Th. Wichert
Technische Physik, Universität des Saarlandes, D-6600 Saarbrücken, Federal Republic of Germany
(Received 23 September 1991)

The perturbed-$\gamma\gamma$-angular-correlation technique (PAC) is a valuable tool for the characterization of defect complexes in crystalline materials. The features of the technique arising in the application to semiconductors are illustrated using the example of ^{111}In-H pairs in Si. This system was studied in the course of an investigation of the passivation of acceptors in Si by H. The consequences of the chemical transmutation of the radioactive probe atoms are discussed. Using Schottky-diode structures, it is shown that PAC is well suited for use in combination with electrical techniques. The PAC technique, which works at any temperature and over a wide range of dopant concentrations, is also sensitive to different charge states of the defect complexes formed. A discussion of the results focuses on the influence of electronic parameters on the electric-field gradient measured at the ^{111}In/^{111}Cd-H pairs in Si.

I. INTRODUCTION

Using radioactive probe atoms, the perturbed-$\gamma\gamma$-angular-correlation technique (PAC) observes microscopic complexes formed between these probe atoms and defects in a host crystal through the modulations in the $\gamma\gamma$-angular-correlation time spectrum with characteristic frequencies. For PAC in semiconductors, defects have been observed via the electric quadrupole interaction. Thus the measured quantity is the electric-field gradient (EFG), being typical for the lattice environment about the probe atom. Using this EFG as a characteristic pattern, the complexes can reliably be recognized and their properties can quantitatively be studied.

PAC studies have been very successful in contributing to the knowledge about defects in metals.[1,2] For this reason the method has also been applied to semiconductors, whose electronic properties are greatly influenced by defects and defect complexes. The number of different probe atoms, however, is rather limited. Using ^{111}In and ^{111m}Cd acting as dopants in elemental,[3-7] III-V,[8,9] and II-VI (Ref. 10) semiconductors information on the complex formation between acceptors or donors on one hand and substitutional or interstitial donors or lattice defects on the other hand has been collected in the past few years. But it should become feasible to employ ^{111}Ag also and perhaps ^{73}As (Ref. 11) as probe atoms in the future.

Of special interest for the study of semiconductors is the need of only a low concentration of probe atoms (typically 10^{16} cm^{-3}) and the possibility of studying the sample at different temperatures. The γ rays are recorded at a distance of several centimeters between sample and detector, so that the sample does not need to be touched. Because at the same time the specimen can be electrically contacted or illuminated, a combination of PAC with electrical or optical measurements is technically feasible and therefore a direct relationship between the formation of microscopic complexes and the resulting changes in electrical or optical properties can be obtained.

In this work the example of ^{111}In-H pairs in Si is used, which have been studied in course of the investigation of the passivation of acceptors in Si by H,[3,4,12-14] in order to discuss new aspects in the characterization of defects arising from the application of PAC to semiconductors. The Cd-H pairs that are detected after the decay of ^{111}In to ^{111}Cd can occur in different electronic and structural states depending on the electronic conditions in the sample. The corresponding change of the characteristic pattern of ^{111}In-H pairs in Si with dopant concentration, degree of passivation, and temperature of the sample is microscopically interpreted. It allows us to infer from the PAC signal the electrically active dopant concentration. The feature of a chemical transmutation of the probe atom is also common to other nuclear techniques such as the Mössbauer effect or β-nuclear magnetic resonance.

PAC experiments at Schottky diodes support the proposed microscopic model through experiments where the PAC signals are reversibly influenced by the applied bias. They show that, in principle, an interesting combination with capacitive techniques should be possible, e.g., deep-level transient spectroscopy (DLTS), which often has problems with the identification of the microscopic origin for an observed level.

II. METHOD

The basic aspects of the method have been described in a recent publication[5] along with a number of examples for PAC investigations in Si using the probe atom ^{111}In. A detailed description of the theory can be found in the work of Frauenfelder and Steffen.[15] Here the essentials of

the theory are briefly summarized and damping effects caused by static inhomogeneity or dynamic fluctuation (also called dynamic relaxation) of the EFG are qualitatively discussed for some basic cases.

Special radioactive probe atoms are required whose decay involves a $\gamma\gamma$ cascade with a number of suitable decay and nuclear parameters. Most frequently used is the isotope ^{111}In (Fig. 1) decaying to an excited nuclear state of ^{111}Cd with a half-life of 2.8 days, which allows for about two weeks of experimental time on one sample. After the chemical transmutation a $\gamma\gamma$ cascade, which brackets an intermediate level of 85-ns half-life, spin $\frac{5}{2}$, and quadrupole moment $Q=0.8b$, deexcites the probe atom to its stable ground state. By a coincidence measurement of the two γ rays under a fixed angle and by recording the time elapsed between them the transition frequencies ω_n are observed, corresponding to an energetic splitting of the intermediate state. This splitting is induced by the interaction between the quadrupole moment of the probe nucleus and the EFG generated by a defect directly associated to the probe atom which perturbs the symmetry of the host lattice about the probe atom.

The constituents of the complex are identified by variation of the experimental conditions and information on the complex geometry and orientation is extracted from the measurement of the EFG tensor. The complex is formed due to an attractive interaction between the ^{111}In atom and the defect, whereas it is detected via its characteristic perturbation of the charge distribution about the residual isotope ^{111}Cd. Hence the electronic or configurational state observed is always that of the "residual" complex containing ^{111}Cd. Usually PAC probe atoms with a half-life of several hours or more undergo such a chemical transmutation. This process can only be avoided by using an isomeric probe atom like ^{111m}Cd available at the isotope-on-line separator ISOLDE at CERN. The half-life of 48 min in this case requires the experiment to be performed at the production place and reduces the number of measurements that can be taken from one sample to maximum two instead of about 20 as in the case of ^{111}In.

The immediate environment of the radioactive probe atom in the host crystal, lattice atoms, defects, and bonds between them, represent an electrical charge distribution. PAC is sensitive to the traceless part of the second spatial derivative of the electrostatic potential, called the electric-field gradient tensor which consists only of three diagonal elements V_{xx}, V_{yy}, and V_{zz} in the principal axes system, where $|V_{xx}| \leq |V_{yy}| \leq |V_{zz}|$. It is completely described by the largest component V_{zz}, measuring the "strength" of the EFG, and the asymmetry parameter $\eta=(V_{xx}-V_{yy})/V_{zz}$, reflecting the deviation of the EFG tensor from axial symmetry ($0 \leq \eta \leq 1$). The symmetry of the EFG corresponds directly to the symmetry of the probe's environment. For a probe atom on a substitutional site in the Si lattice the EFG vanishes ($V_{zz}=0$) and a point defect located on a highly symmetric neighbor site produces a perturbation ($V_{zz} \neq 0$) whose axial symmetry is reflected by $\eta=0$. The EFG of complexes without axial symmetry are characterized by a nonzero asymmetry parameter $0<\eta \leq 1$. Perturbations of the lattice outside the first few shells about the probe atom do not lead to a strong and well-defined EFG mainly because its strength decreases with r^{-3}, denoting by r the distance between defect and probe atom.

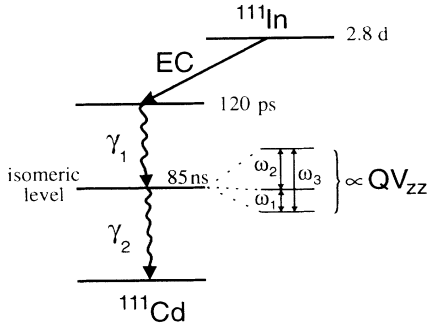

FIG. 1. Nuclear decay scheme of the PAC probe atom ^{111}In decaying to ^{111}Cd via electron capture (EC). The hyperfine splitting of the isomeric level of ^{111}Cd populated by the first γ transition is used in the measurement of the electric-field gradient.

Using a standard PAC setup in "slow-fast coincidence" technique[16] with four detectors surrounding the sample, which is doped with the probe atoms (^{111}In in our case), the correlation in space and time of the two γ quanta of the same decay event is recorded. For all possible combinations of detectors (angular information) the time between two correlated γ transitions is measured and stored. In this way 12 time spectra are collected that are combined to a single time spectrum $R(t)$, containing only the hyperfine interaction between the quadrupole moment Q of the probe nucleus and the EFG of the lattice environment. $R(t)$ has the form

$$R(t)=A\sum_i f_i G_i(t) , \tag{1}$$

with the perturbation factor $G(t)$ for pure electric quadrupolar interaction

$$G(t)=\sum_{n=0}^{3} S_n \cos(\omega_n t) , \tag{2}$$

where the anisotropy A is a nuclear parameter of the decay folded with the angular resolution of the setup, giving $A=-0.13$ in the experiments discussed here. Several fractions of probe atoms f_i ($\sum_i f_i=1$) may experience different EFG's with strengths V_{zz}^i, described by the quadrupole coupling constant $\nu_Q=eQV_{zz}/h$. In the case of ^{111}Cd, because of the $\frac{5}{2}$ spin of the intermediate level, for every EFG, three transition frequencies ω_n occur with the simple relationship $\omega_n=n(3\pi/10)\nu_Q$ ($n=1,2,3$) in case of axial symmetry. The amplitudes of the transition frequencies S_n depend on the orientation of the main axis of the EFG with respect to the detector system and the time resolution of the setup (about 2 ns). The first dependence is used to determine the orientation of the formed probe atom defect complex with respect to the host lattice.

As an illustration PAC spectra and their Fourier transforms for some basic situations are displayed in Fig. 2. In

case (a) 100% of the probe atoms are exposed to a zero EFG, which is expected if all probe atoms are on substitutional sites and fourfold coordinated in the Si lattice. The spectrum is described by the straight line $R(t)=A$. In (b) 100% of the probes experience the same unique, axially symmetric EFG as produced by a trapped defect forming a well-defined complex. Pronounced oscillations occur and the Fourier transform shows the three transition frequencies ω_n. The complex is tagged by the values of ν_Q and η (characteristic pattern), which allow its reliable recognition in any experimental situation. Inhomogeneities of the EFG in space or time both effect a different type of damping of the PAC signal with increasing time. In Fig. 2(c) a Gaussian-shaped static distribution of EFG's around a mean value with the width σ is assumed, leading to an attenuation term in

$$G_{\text{static}}(t)=\sum_{n=0}^{3} e^{(-n\sigma t)^2} S_n \cos(\omega_n t) , \tag{3}$$

damping preferentially the higher transition frequencies. In the Fourier transform the corresponding broadening of the lines is shown, which for ω_2 and ω_3 is two and three times as large as for ω_1, respectively. For long times $R(t)$ approaches the so-called "hard-core" value S_0.

In Fig. 2(d) the EFG fluctuates in strength or orientation with a rate that is fast compared to the frequencies ω_n. Then a well-defined time average of ν_Q is observed. All three frequencies are equally damped and their Fourier lines are equally broadened:

$$G_{\text{dynamic}}(t)=e^{-\lambda t}\sum_{n=0}^{3} S_n \cos(\omega_n t) . \tag{4}$$

The relaxation parameter λ becomes smaller the faster the fluctuations occur. In this case of dynamic relaxation, the hard-core value S_0 is also affected and for long times $R(t)$ approaches zero.

In this way, via the relative broadening of the frequencies ω_n and the attenuation of S_0, pure static and pure fast dynamic damping effects can be distinguished. In addition, dynamic processes in the intermediate range of fluctuation rates can be treated, as demonstrated by the work of Achtziger.[17] Since in this case the Fourier lines are also broadened differently, discrimination between static and dynamic processes based on the measured spectra is rather difficult.

By fitting the spectra with the theoretical function (1), the absolute fractions of probe atoms f_i (detection limit approximately 1%), the associated quadrupole coupling constants ν_Q, the symmetry (from the frequency ratios

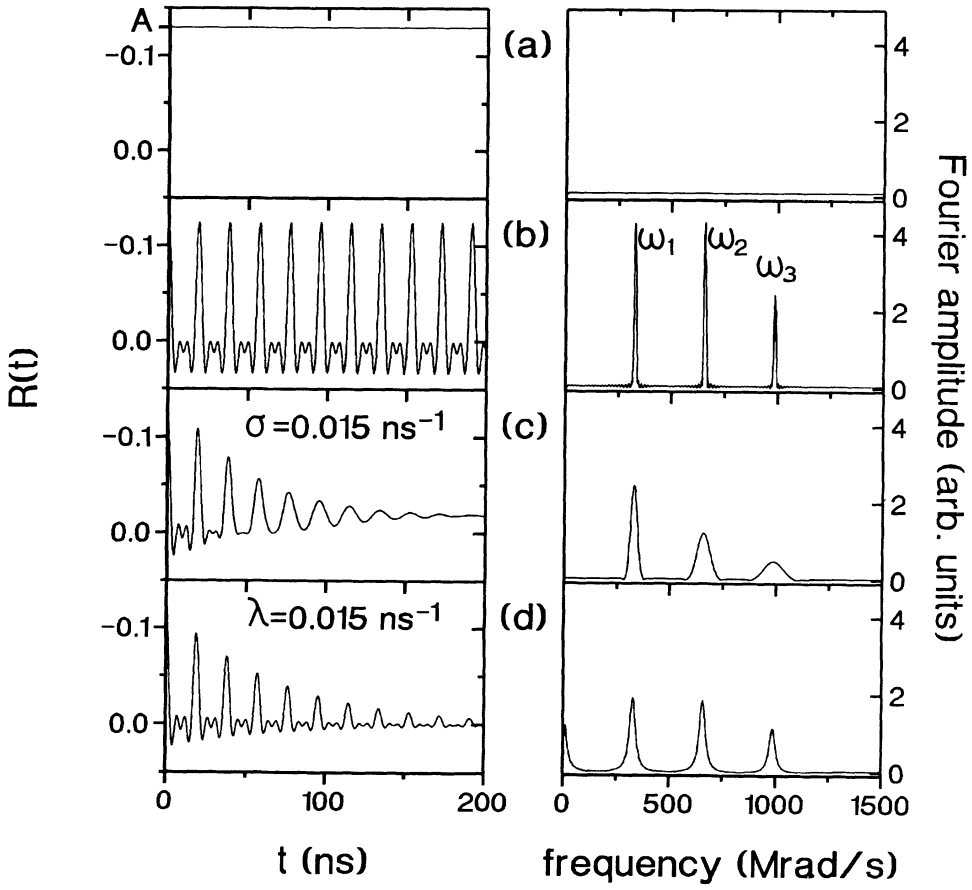

FIG. 2. Theoretical PAC spectra (left) and their Fourier transforms (right) for (a) for $\nu_Q=0$, (b) $\nu_Q=349$ MHz without damping, (c) with static damping ($\sigma=0.015$ ns^{-1}) due to a distribution of ν_Q about 349 MHz, and (d) with dynamic relaxation ($\lambda=0.015$ ns^{-1}) due to a fluctuation of ν_Q about the mean value of 349 MHz.

$\omega_2{:}\omega_1$), and the orientation of the EFG's (from the amplitudes S_n) can be extracted. For the system of ^{111}In-H pairs in Si, electronic inhomogeneities are inherent (see Fig. 4), leading to static damping effects because of static EFG distributions as discussed later. Because the type of attenuation (pure static or mixed static and dynamic) could not be unambiguously identified, a minimum set of free parameters was used to obtain a satisfactory fit and dynamic processes were not considered. Since the fractions f_i and coupling constants ν_Q are rather insensitive to the type of attenuation parameter used, this restriction is uncritical for the results discussed here. The analysis also takes into account the reduction of amplitudes of high frequencies by the time resolution of the setup.

The chemical transmutation of the probe nucleus has consequences for the electronic structure of the atom and the environment. After the formation of an In-H pair during sample preparation, the ^{111}In converts to ^{111}Cd by electron-capture decay (Fig. 3). The resulting inner hole in the atomic shell relaxes very fast by Röntgen and Auger processes, the latter creating further holes and leaving behind a highly ionized Cd atom. The multiple ionization is reduced by capture of electrons from the surrounding lattice. Since unique and well-defined PAC signals of H atoms trapped at ^{111}In are observed at ^{111}Cd (see, e.g., Fig. 9), obviously the ^{111}Cd probe atom and the complex reach a stable equilibrium electronic and structural state in less than 120 ps, the half-life of the excited state of ^{111}Cd created by the decay of ^{111}In. Otherwise the signals would be completely destroyed by the great changes of the EFG coming along with a decaying ionization of the probe atom or a structural reconfiguration during the time window of the isomeric nuclear level of ^{111}Cd. In this time window the complex contains Cd, which is a group II element. For In-H pairs the acceptor state of In is removed from the gap by the H passivation, but the Cd-H pair again has acceptor character, as supported by simple valence considerations. Depending on Fermi-level position and temperature of the crystal, this acceptor can be ionized or neutral, resulting in different well-defined EFG's, which in turn enables the microscopically sensitive PAC to trace back to the macroscopic electronic conditions in the sample.

III. EXPERIMENTAL PROCEDURE

The radioactive probe atoms are usually implanted with 350 keV into homogeneously B-doped Si wafers, leading to a Gaussian depth profile centered at 1640 Å with a width of 470 Å and a peak concentration of about 5×10^{16} cm^{-3}. To remove the implantation-induced lattice damage and to activate the ^{111}In acceptors, the samples were annealed at 1173 K either for 10 min in a furnace or for 20 s in a rapid thermal annealing setup. Passivation of the samples by H was performed in a H plasma, with help of a low-energy ion separator (200 eV), or simply by boiling in H_2O. All three procedures lead to the formation of the identical In-H pairs. Isochronal annealing (10 min) was performed in air up to 523 K and under flowing N_2 gas above this temperature. Schottky contacts with a diameter of 7 mm, necessary to cover the implantation spot of 5 mm, were prepared by Ti evaporation under high vacuum conditions by means of an electron gun. The back contacts consisted of a liquid In-Ga mixture.

Of importance for the interpretation of the experimental data are the electronic inhomogeneities in the surface region of the sample, qualitatively shown in Fig. 4. In addition to the basic B doping of the crystal the probe atoms represent an electrically active acceptor profile. The acceptor atoms are partially passivated by H atoms penetrating from the surface. For samples with a not-too-high electrically active acceptor concentration the band bending induced by surface states or by an applied bias reaches the region of the implanted probe atoms. The resulting variation of the Fermi level across the profile of the probe atoms causes the charge state of the Cd-H acceptors to depend on depth and thereby induces a static superposition of different PAC signals that reflect the electronic inhomogeneities.

IV. ELECTRIC-FIELD GRADIENTS OF ^{111}In-H PAIRS IN Si

As already mentioned above, the PAC signal of ^{111}In-H pairs in Si depends on the electronic state of the sample. As a function of dopant concentration and temperature different EFG's are measured at ^{111}Cd for the same complex, which is unambiguously identified as ^{111}In/^{111}Cd-H pair.[3] These EFG's have been observed due to a contamination of their Si samples with H by Kemerink and Pleiter[18] who, however, did not yet identify them as caused by pairing of ^{111}In with H atoms. Depending on the experimental conditions structurally and/or electronically different states of the complex are formed, leading

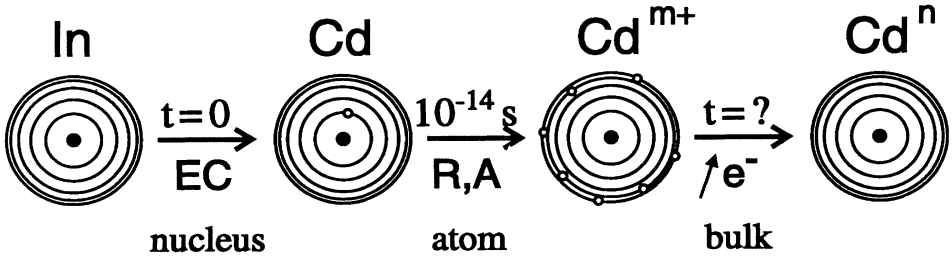

FIG. 3. Schematic representation of the consequences for the electronic shell of the probe atom caused by the decay of ^{111}In to ^{111}Cd via electron capture (EC). The transmutation of the nucleus generates a hole in the electronic shell of the residual atom ^{111}Cd that relaxes via Röntgen (R) and Auger (A) processes, the latter leading to a multiple positive ionization. The surrounding Si crystal determines the final charge state n of the probe atom or complex in equilibrium.

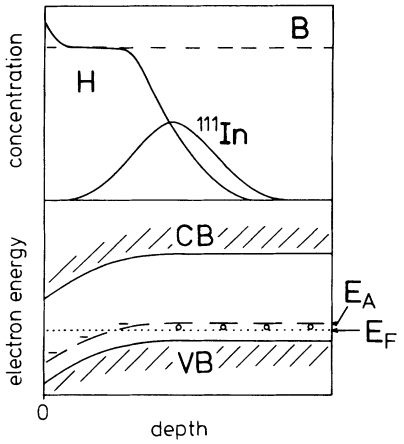

FIG. 4. Schematic representation of possible electronic inhomogeneities in a Si sample. The implantation of ^{111}In produces a Gaussian depth profile of probe atoms in the Si crystals which are homogeneously doped with B (dashed line) at different concentrations. The concentration of H, diffusing in from the surface decreases with depth (top). The bands of the p-type Si are bent downwards by the influence of surface charges producing a space-charge region with localized acceptors (level E_A) which is depleted of free holes (bottom).

to differing charge distributions about the probe atom at the time of the measurement and hence to different EFG's. The nomenclature and symbols used in the following are collected in Table I.

Figure 5(a) qualitatively summarizes the experimental results presented in IV A. The coupling constants ν_Q, as extracted from samples with utmost homogeneous electronic conditions (Fig. 4), are plotted against the temperature and the electrically active, which means not by H passivated, part of the B concentration of the sample. The lower, vaulted surface in Fig. 5(a) shows that for low temperature and high B concentration (open circles), a coupling constant $\nu_{Q1/0}$ of 269 MHz is observed, which for increasing temperature and decreasing B concentration is continuously shifted to $\nu_{Q1/-}=349$ MHz (at 300 K; solid circles). This transition correlates well with the shift of the Fermi level in the sample [Fig. 5(b)], expected to occur for this change of B concentration and temperature, from near the valence band towards the middle of the band gap. Therefore the observed frequency shift is assigned to a charge transition at the Cd-H pair,[4] which is acting as a shallow acceptor and is characterized by $\nu_{Q1/0}=269$ MHz in the neutral charge state $(\text{Cd-H})^0$ and by $\nu_{Q1/-}=349$ MHz in the ionized state $(\text{Cd-H})^-$.

Besides the surface for ν_{Q1} described above, there is an additional state of the complex characterized by $\nu_{Q2}=463$ MHz (value at 300 K; solid triangles) occurring in samples with low electrically active B concentration, i.e., in almost intrinsic or highly passivated material, and preferentially at low temperatures. It is observed in coexistence with $\nu_{Q1/-}=349$ MHz (300 K), which is dominant at 300 K. On lowering the temperature, the fraction f_2 of ν_{Q2} grows at the expense of the fraction $f_{1/-}$ of $\nu_{Q1/-}$ until the latter disappears below 80 K. For the coupling constant ν_{Q2} only a slight variation with temperature is observed which corresponds to the normal temperature dependence of the EFG caused by lattice vibrations. The population of the two flat "coupling-constant surfaces" on the left edge of the figure is qualitatively described by the size of the corresponding symbols. The occurrence of the state ν_{Q2} cannot be correlated with the position of the Fermi level and is therefore ascribed to a second, structurally different configuration *(Cd-H) of the Cd-H complex. The only electronic parameter f_2 is consistently correlated with is the free-hole concentration in the respective volume of the sample. The fraction f_2 is dominant for low-hole concentration, i.e., for low acceptor concentration and low temperature, and disappears if the concentration of holes in the sample increases. The population of the two states $\nu_{Q1/-}$ and ν_{Q2} was already studied by Kemerink and Pleiter[18] for differently doped Si and several temperatures. Their results fit nicely to the data presented here and always show a preferential population of ν_{Q2} for low-hole concentration.

TABLE I. The chemical nature of the different complexes along with their electronic states, their coupling constants at 300 K, and the symbols used in the figures are summarized. The superscript following the parentheses denotes the charge state and the asterisk in front of the parentheses a second structural configuration of the Cd-H pair. Summing up the fractions of all Cd-H states yields the fraction of In-H pairs present in the sample. [In earlier publications (Refs. 3, 12, and 13) $\nu_{Q1/-}$ was referred to as ν_{Q1} and $\nu_{Q1/0}$ and ν_{Q3}. Kemerink and Pleiter (Ref. 18) denoted $\nu_{Q1/-}$ by "No. 328" and ν_{Q2} by "No. 433."]

Complex	State	Coupling constant at 300 K	Symbol
In/Cd-H	$1=(\text{Cd-H})^{-w}$	$\nu_{Q1}=269$–349 MHz, depending on degree of ionization $0\le w\le 1$	○
	Extremes		
	$1/0=(\text{Cd-H})^0$	$\nu_{Q1/0}=269$ MHz	○
	$1/-=(\text{Cd-H})^-$	$\nu_{Q1/-}=349$ MHz	●
In/Cd-H	$2=*(\text{Cd-H})$	$\nu_{Q2}=463$ MHz	▼
In-H		Sum of all Cd-H states	■

A. Experimental results

In Fig. 6(a) the dependence of the measured coupling constants on sample temperature and B concentration are quantitatively shown. These experimental curves represent cross sections of the surfaces in Fig. 5(a). In originally intrinsic samples that are electrically dominated by the doping with the ^{111}In probe atoms the coupling constants $\nu_{Q1/-}=349$ MHz and $\nu_{Q2}=463$ MHz are both observed. Their values slightly increase towards lower temperatures, as expected from the influence of lattice contraction of the host crystal. For the intrinsic sample Fig. 6(b) shows the populations of the two coupling constants. At room temperature the fraction f_2 of ν_{Q2} is smaller than $f_{1/-}$ of $\nu_{Q1/-}$ and it grows at the expense of $f_{1/-}$ for decreasing sample temperature until $\nu_{Q1/-}$ is no longer observable below 80 K. During this reversible repopulation the sum of the fractions $f_{1/-}$ and f_2 is not strictly constant but becomes smaller at low temperatures.

If the B concentration dominates over the probe atom concentration solely, the coupling constant $\nu_{Q1/0}$ occurs at low temperature and ν_{Q2} is not observed [Fig. 6(a)]. Depending on the amount of electrically active B acceptors with rising temperature, ν_{Q1} continuously increases towards $\nu_{Q1/-}$. This transition occurs at lower temperatures if the B concentration in the sample is reduced. In the transition regime between $\nu_{Q1/0}$ and $\nu_{Q1/-}$ a pronounced damping of the PAC signal is observed, as it is visible in the $R(t)$ spectra and the Fourier transforms of Fig. 7. It shows for a sample doped with 5.5×10^{17} B cm^{-3} measurements between 10 and 300 K. Whereas the signal of $\nu_{Q1/0}$ is undamped at 80 K, the shift of the cou-

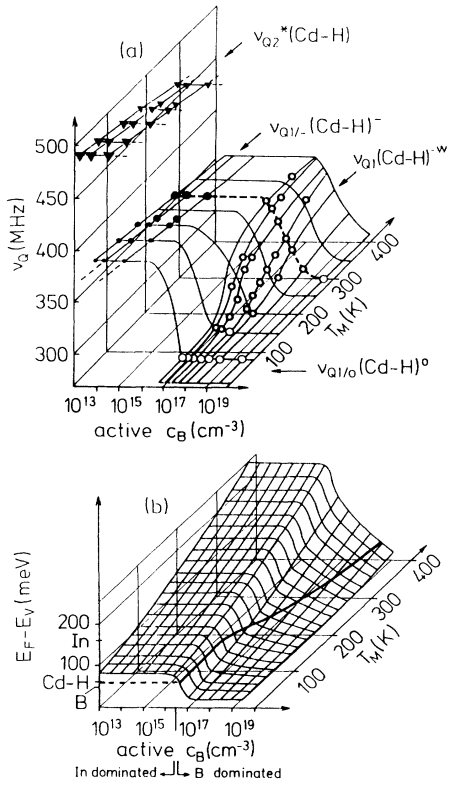

FIG. 5. (a) Measured quadrupole coupling constant ν_Q of ^{111}In/Cd pairs in Si as a function of sample temperature T_M and electrically active B concentration c_B. The lower surface shows a continuous transition from $\nu_{Q1/0}=269$ MHz to $\nu_{Q1/-}=349$ MHz for increasing temperature and decreasing B concentration. Between the upper surface and the left part of the lower one, for In-dominated samples a repopulation from $\nu_{Q2}=463$ MHz to $\nu_{Q1/-}$ is observed with increasing temperature. Here the different fractions of probe atoms are represented by the size of the symbols. The values of the three coupling constants $\nu_{Q1/0}$, $\nu_{Q1/-}$, and ν_{Q2} refer to $T_M=300$ K. The symbols are defined in Table I. The right superscript at the (Cd-H) pair (0, −, or $0<w<1$) refers to the charge state and *(Cd-H) means a second, presumably structurally different, configuration of the complex. (b) Calculated Fermi level determined by the In and B doping of the samples with respect to the valence band as a function of the same parameters as in (a). If the Fermi level increases over the acceptor level of the Cd-H pair (bold line) it becomes negatively ionized and the coupling constant continuously changes from $\nu_{Q1/0}$ to $\nu_{Q1/-}$ [compare (a)]. Due to the softening of the Fermi distribution the transition is less steep for higher temperatures. For the calculation plotted in the figure additional to the B concentration a homogeneous In doping of 10^{16} cm^{-3} was assumed to take into account the electrical activity of the probe atoms. For any given acceptor concentration and temperature the Fermi level was calculated numerically from the condition of charge neutrality.

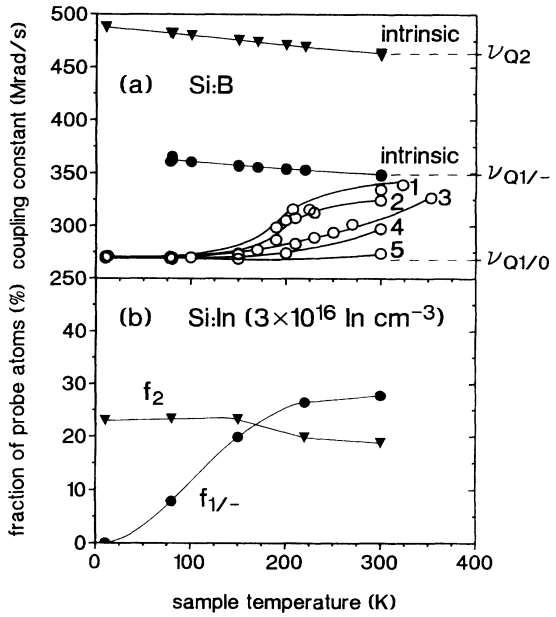

FIG. 6. (a) Transition of the quadrupole coupling constant ν_{Q1} from $\nu_{Q1/0}$ to $\nu_{Q1/-}$ with increasing sample temperature for differently B-doped Si. The electrically active B concentration (deduced from Fig. 8) and the total B concentration (in parentheses) of the samples are 1: 0.88×10^{17} cm^{-3} (5.5×10^{17} cm^{-3}), 2: 1.7×10^{17} cm^{-3} (5.5×10^{17} cm^{-3}), 3: 3.3×10^{17} cm^{-3} (5.5×10^{17} cm^{-3}), 4: 0.65×10^{18} cm^{-3} (2.1×10^{18} cm^{-3}), 5: 3.0×10^{18} cm^{-3} (5.0×10^{18} cm^{-3}). In intrinsic samples $\nu_{Q1/-}$ and ν_{Q2} slightly increase to lower temperatures. Below 80 K $\nu_{Q1/-}$ is not observed. (b) Fractions $f_{1/-}$ and f_2 of $\nu_{Q1/-}$ and ν_{Q2} as a function of sample temperature for low-In-doped Si. Intrinsic samples, which are dominated by the doping of the In probe atoms, show the same behavior.

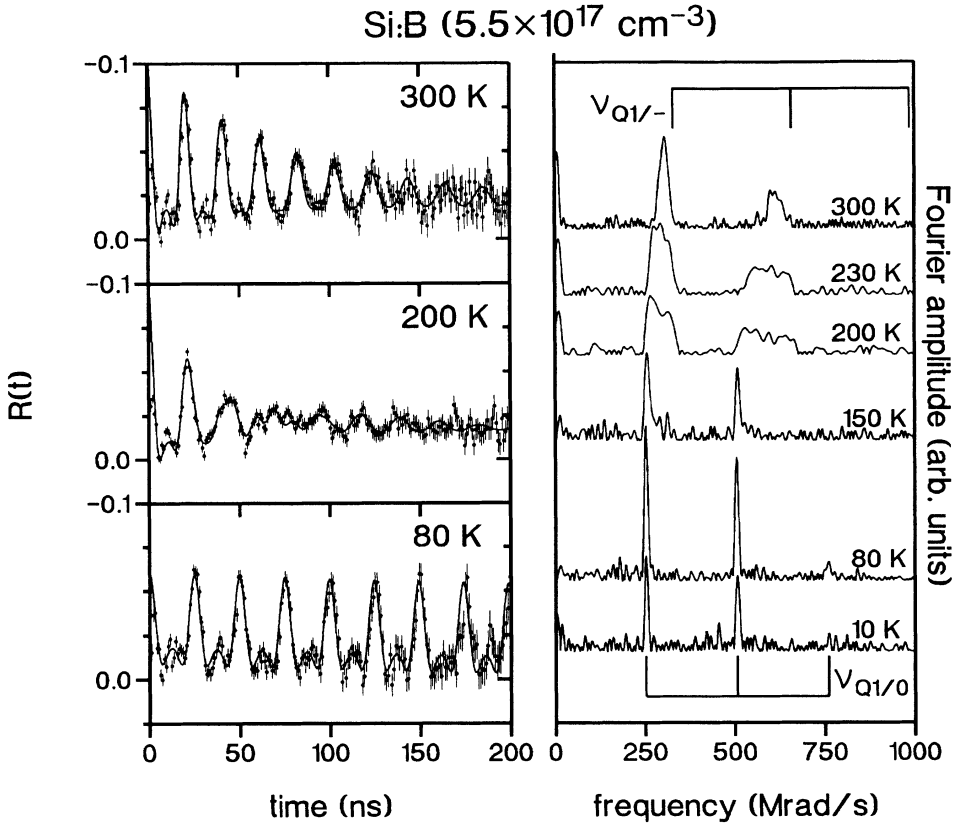

FIG. 7. For Si doped with 5.5×10^{17} B cm^{-3}, PAC spectra (left) and Fourier transforms (right) of ^{111}In/Cd-H pairs measured at different temperatures. During the continuous transition of ν_{Q1} from $\nu_{Q1/0}$ to $\nu_{Q1/-}$, due to the electronic inhomogeneities in the surface layer of the sample, a pronounced static damping occurs around 200 K.

pling constant towards $\nu_{Q1/-}$ with increasing temperature is accompanied by an increasing attenuation, visible in the faster damping of the $R(t)$ function and the broadening of the Fourier lines. The attenuation parameter reaches a maximum around 200 K and decreases again above this temperature when the coupling constant approaches $\nu_{Q1/-}$, whose value is not completely reached in this case.

The dependence of the coupling constant ν_{Q1} of ^{111}In/Cd-H pairs on the concentration of electrically active B atoms, which was varied by the dissociation of B-H pairs during an isochronal annealing program, is shown in Fig. 8. After implantation of ^{11}In and annealing of the irradiation induced damage the samples were passivated with H by means of low-energy H^+ implantation or by boiling in H_2O. The fractions of In forming In-H pairs (not shown here) and their coupling constants were measured at 300 K after each annealing step. For samples with a very low B concentration ("intrinsic") $\nu_{Q1/-}$ and ν_{Q2} are observed, remaining constant up to 450 K until all In-H pairs are dissociated. In high-B-doped Si, the same intrinsic coupling constants appear after passivation. But, during annealing ν_{Q2} disappears and ν_{Q1} shifts to lower values. For each B-doping level ν_{Q1} reaches a characteristic value when all acceptors are reactivated. These asymptotic values of ν_{Q1} measured for different B concentrations enter Fig. 5(a) for the temperature of 300 K (dashed line). This dependence of ν_{Q1} on the B concentration has been used to determine the electrically active B concentration of the partly passivated samples shown in Fig. 6(a) by comparing the measured value of ν_{Q1} at

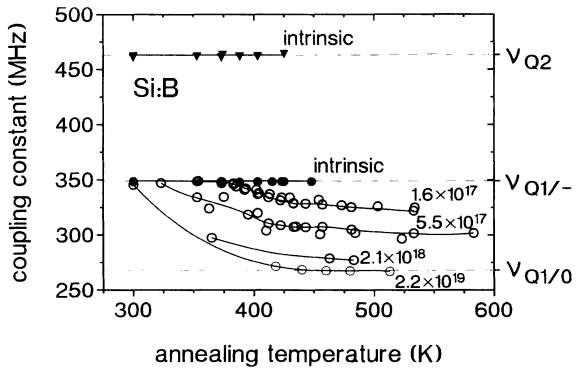

FIG. 8. Measured quadrupole coupling constants for ^{111}In/Cd-H pairs in Si doped with B at different concentrations as a function of the annealing temperature and hence also of the concentration of electrically active B atoms. For intrinsic samples $\nu_{Q1/-}$ and ν_{Q2} remain constant. For higher B concentrations ($>10^{17}$ cm^{-3}) the decay of the passivation causes the disappearance of ν_{Q2} and a transition from $\nu_{Q1/-}$ to a lower value of ν_{Q1}, which is typical for each B concentration.

300 K; the corresponding B concentrations are given in the figure caption. With help of these concentrations of electrically active B atoms, the curves for ν_{Q1} as a function of sample temperature were incorporated in Fig. 5(a).

All EFG's observed for ^{111}In/Cd-H pairs are axially symmetric along ⟨111⟩ axes of the Si lattice. The axial symmetry is obvious from the measured frequency ratios $\omega_2:\omega_1=2$ and the ⟨111⟩ orientation from the typical dependence of the amplitudes S_n of each EFG on the orientation of the γ detectors with respect to the lattice of the Si crystal, shown in Fig. 9: S_2 and S_3 are small if the γ detectors are set along ⟨111⟩ lattice directions.

B. Discussion

Assuming the ^{111}Cd atom to stay after the decay on the substitutional site previously occupied by the parent ^{111}In, for the H atoms all sites on the ⟨111⟩ axis in the nearest neighborhood of the probe atom have to be considered (Fig. 10). The axial symmetry and the ⟨111⟩ orientation of the EFG's are time-averaged properties of the complex, because fluctuations on time scales $t \ll (\nu_Q)^{-1}$ cannot be resolved. If the structure of the Cd-H complex is different from that of the original In-H complex, a possible reconfiguration has to be completed within less than 1 ns even at temperatures as low as 10 K, otherwise the well-defined PAC signals would be destroyed. Based on cluster calculations for B-H pairs the bond-centered site between the B and a neighboring Si atom is favored for the H atom (e.g., Refs. 19 and 20).

Analogous to a model of Forkel *et al.*[21] and suggested by Baurichter *et al.*,[4] the shift of the coupling constant between $\nu_{Q1/0}=269$ MHz, and $\nu_{Q1/-}=349$ MHz [Fig. 5(a), lower surface] can be well understood by a charge transition at the observed Cd-H pair. The In acceptor atom is electrically passivated by trapping of a H atom. The radioactive decay changes the valence and a simple consideration suggests that the double acceptor Cd is only singly passivated by one H atom which leads to a shallow single acceptor behavior of the complex. For a low Fermi level (low temperature, high B concentration) the complex is neutral, designated as $(\text{Cd-H})^0$, and is characterized by the coupling constant $\nu_{Q1/0}=269$ MHz. For a Fermi level higher than the gap level of the complex [bold line in Fig. 5(b)], the complex becomes negatively charged. Because the charge distribution about the probe atom is altered by the additional electron in $(\text{Cd-H})^-$, the EFG changes and the coupling constant rises to $\nu_{Q1/-}=349$ MHz. In the intermediate range the charge state of the complex is neither neutral (0) nor negative (−) but fluctuates, so that the averaged coupling constant ν_{Q1} is observed:

$$\nu_{Q1}=w\nu_{Q1/-}+(1-w)\nu_{Q1/0}\,, \tag{5}$$

where w is the probability for the population of the ionized state, which is determined by the position and the sharpness of the Fermi distribution. The level of the Cd-H pair $E_{\text{Cd-H}}$ has to lie between the levels of B (E_V+45 meV) and In (E_V+160 meV), because the ionization of the complex is completely controlled by these dopants: If the B concentration exceeds the local ^{111}In doping by the probe atoms (about 10^{16} cm^{-3}) $\nu_{Q1/0}$ is observed and for B doping being lower than the local ^{111}In concentration $\nu_{Q1/-}$ occurs. From the temperature dependence of ν_{Q1} in B-doped samples $E_{\text{Cd-H}}$ has been determined by Gebhard *et al.*[22] to be 60(10) meV above the valence band. This value agrees well with our result of 59(4) meV obtained from Si doped with Ga by implantation, where the electrically active Ga concentration was determined

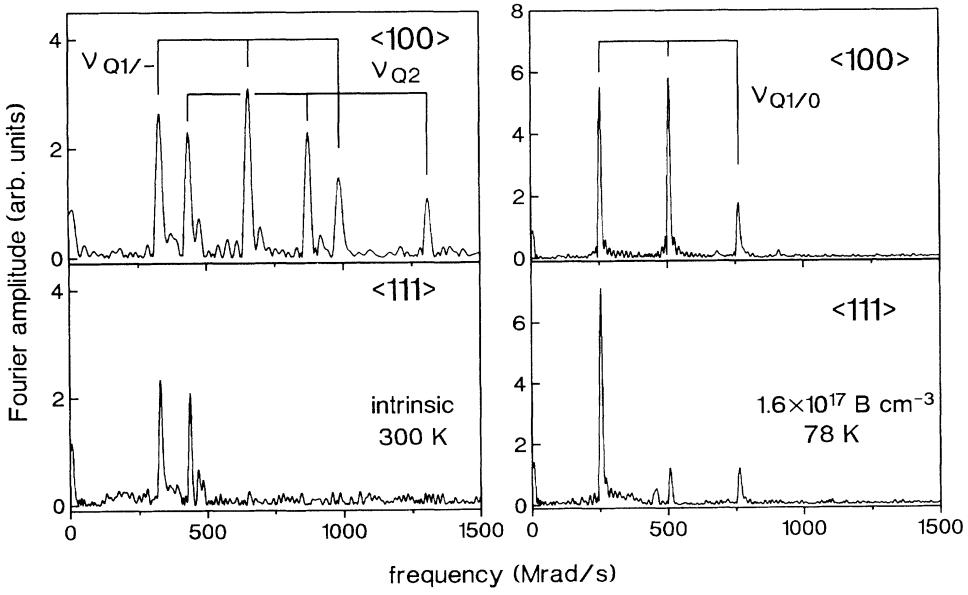

FIG. 9. Fourier spectra of ^{111}In/Cd-H pairs in intrinsic Si measured at 300 K (left) and in B-doped Si at 78 K (right) with detectors along ⟨100⟩ (top) and ⟨111⟩ (bottom) lattice directions. For all triplets holds $\omega_2:\omega_1=2$ and the amplitudes of ω_2 and ω_3 become small for detectors along ⟨111⟩ directions, what indicates axial ⟨111⟩ symmetry of the complexes.

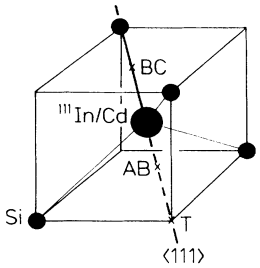

FIG. 10. Possible lattice sites of H within an acceptor-H pair in Si fulfilling axial ⟨111⟩ symmetry: bond centre site (BC) on the bond between the acceptor and a Si atom, antibonding site (AB) on the opposite side of a bond, and tetrahedral site (*T*).

by resistivity measurements for different degrees of passivation and the corresponding change of ν_{Q1} was pursued by PAC.[23]

Within this model the transitions in Figs. 6 and 5(a) between $\nu_{Q1/0}$ and $\nu_{Q1/-}$ as a function of temperature are explained by the rise of the Fermi level above $E_{\text{Cd-H}}$ happening at lower temperature for lower B concentration [see Fig. 5(b)]. In Fig. 8 the acceptor doping of the samples is highly passivated immediately after H loading and the formed ^{111}In/Cd-H pairs reside in an intrinsic appearing region, which is reflected by the occurrence of $\nu_{Q1/-}$ and ν_{Q2}. During annealing B-H and In-H pairs dissociate, thereby increasing the electrically active acceptor concentration and lowering the Fermi level. The state ν_{Q2} vanishes because of the increasing hole concentration and $\nu_{Q1/-}$ drops towards $\nu_{Q1/0}$ because of the decreasing degree of ionization of the Cd-H pair. For each B concentration at 300 K a characteristic minimum value of ν_{Q1} is assumed which corresponds to a minimum Fermi level reached for complete reactivation of the acceptors.

The PAC signal is sharp and shows no damping for the extreme values $\nu_{Q1/0}$ and $\nu_{Q1/-}$. The damping observed in the transition regime appears to be dominantly static, as is evident from the ratio of the broadening of the three Fourier lines of 1:2:3 [compare Figs. 7 and 2(c)]. This damping is caused by the surface band bending reaching into the region of the probe atoms and producing a local variation of the Fermi level with respect to the (Cd-H) acceptor level (see Fig. 4). Accordingly, the charge state of the complex varies slightly with depth leading to a static distribution of EFG around a mean value ν_{Q1}. Additionally, a dynamic relaxation might occur if the rate of the charge fluctuation is not large compared with ν_{Q1}. However, as mentioned above, a quantitative analysis of a possible dynamic relaxation in addition to the static damping does not seem to be of experimental significance because of the similarity of the effects of the different types of attenuation parameters on the fitted theory function.

The state ν_{Q2} only occurs in samples with low acceptor concentration and preferably at low temperature. Presumably, it has to be identified with a structurally different configuration *(Cd-H) of the Cd-H pair, whose equilibrium population is controlled by the concentration of free holes. It cannot be distinguished whether the two structural configurations observed at the Cd atom exist already at the In atom or whether a single, unique configuration of the In-H pair develops into two structurally different Cd-H configurations. For ν_{Q2} under none of the numerous experimental conditions has a damping been observed. This fact might indicate that the In-H pair already exists in two different configurations whose populations depend on the concentration of free holes.

C. Application

The characteristic dependence of the EFG's or ν_{Q1} values associated with the ^{111}In-H or Cd-H pairs on the Fermi level can be used to determine the electrically active acceptor concentration in the region where the ^{111}In/Cd-H pairs reside. In Fig. 11 (left panel) for different B concentrations the asymptotic experimental values of ν_{Q1} measured at 300 K have been used to plot the position of the Fermi level against the corresponding value of ν_{Q1}. In the right panel the calculated Fermi level is plotted for different acceptor species and concentrations. The diagram allows us to read out the concentration of electrically active acceptor atoms via the Fermi-level dependence of ν_{Q1}, provided that the chemical species of the acceptor is known. Qualitatively, a rising coupling constant signals an increasing passivation and vice versa.

The role of the inhomogeneity of the H passivation with depth and its appearance in the PAC spectra is illustrated in Fig. 12, where the Fourier transform of a PAC spectrum taken at 10 K at a sample doped with 1.6×10^{17} B cm^{-3} is shown. Predominantly ν_{Q2}, characteristic for intrinsic samples at this temperature, is observed with a fraction of 40%. In addition $\nu_{Q1/0}$, typical for a high electrically active B concentration, occurs with a fraction of 20%. As sketched in the inset of Fig. 12, obviously during H loading in boiling H_2O a completely passivated surface layer, covering about 40% of the ^{111}In profile, had been produced from where ν_{Q2} arises. In the next layer the B doping is only partly passivated leading to the observation of $\nu_{Q1/0}$ at 10 K, whereas no H reached the remaining ^{111}In atoms deeper in the sample. In this way the degree of passivation and the H depth profile can be qualitatively pursued during the PAC experiment.

D. Summary

It has been shown that the PAC signal of ^{111}In/Cd-H pairs is rather complex but phenomenologically completely characterized and mainly understood. A detailed knowledge of this characteristic signature makes it impossible to mix up In-H pairs with other In-defect complexes. Furthermore, it is possible to qualitatively conclude from the measured coupling constant on the electronic conditions of the sample (Fermi-level position, electrically active acceptor concentration) and their inhomogeneities caused by the H passivation profile. Whereas the structural information is affected by the radioactive decay of ^{111}In to ^{111}Cd, this process does not touch the information on the formation conditions and on the thermal stability of In-H pairs, which is presented

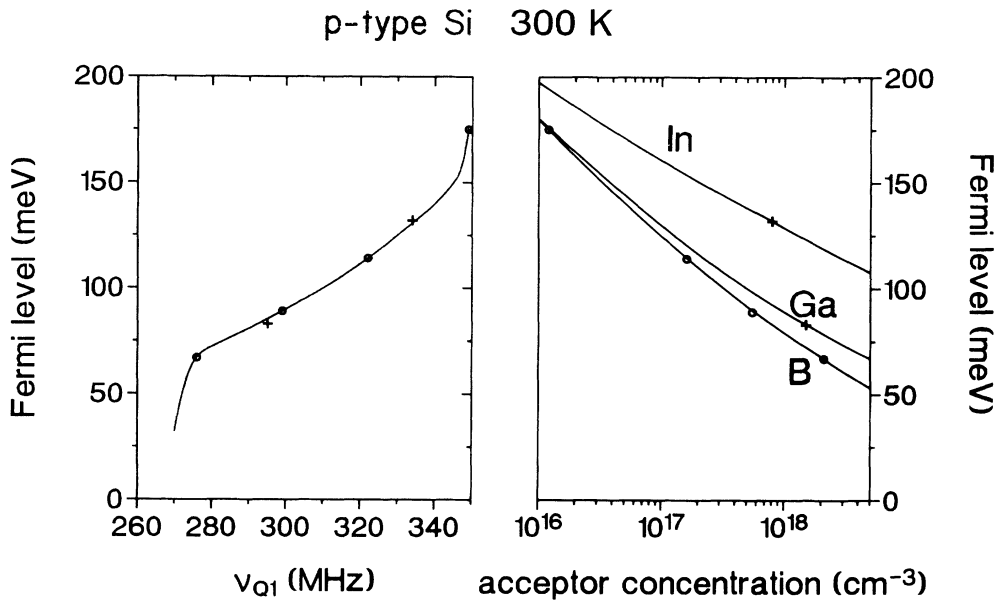

FIG. 11. Fermi-level dependence of the quadrupole coupling constant ν_{Q1} at 300 K. The Fermi level calculated from the condition of charge neutrality for different acceptor concentrations and species is shown on the right-hand side. On the left-hand side the calculated Fermi level for some B concentrations is plotted against the corresponding measured values of ν_{Q1} (circles, taken from Fig. 8) and complemented by a spline curve. Using the measured value of ν_{Q1}, the actual electrically active acceptor concentration of B, Ga, or In can be read out via the Fermi level from the diagram. A test for two samples doped with In and Ga, respectively, by implantation shows good agreement (crosses) (Ref. 23).

elsewhere:[14] The Cd-H pairs can only be observed if they were already formed at the In atoms, and they only disappear if H has already dissociated from the In atoms in a preceding annealing step.

V. EXPERIMENTS IN SCHOTTKY DIODES

The interpretation given above explains the different observed EFG's associated with the formation of ^{111}In/Cd-H pairs in terms of populations of different electronic and structural states of Cd-H pairs depending on electronic equilibrium parameters of the semiconductor

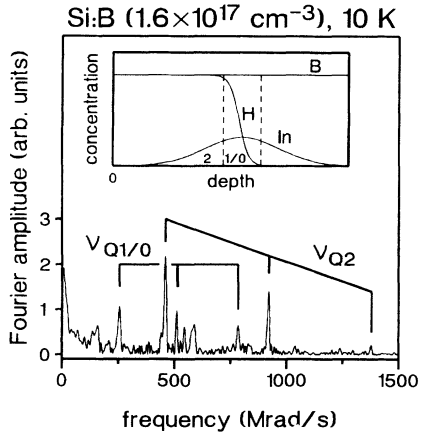

FIG. 12. Fourier spectrum of a measurement at 10 K at a Si sample with 1.6×10^{17} B cm^{-3} which was inhomogeneously passivated with H. The coupling constants ν_{Q2} and $\nu_{Q1/0}$ are observed simultaneously, arising from a highly and a partly passivated layer of the sample, respectively (see inset).

(Fermi level, free-hole concentration). In order to test the interpretation it would be desirable to vary reversibly these parameters at constant temperature and without changing the dopant concentration or the degree of passivation of the sample. This is possible in the space charge region of a Schottky diode as shown in Fig. 13. By applying a bias to the diode, the Fermi-level position and correspondingly the concentration of free holes is influenced up to certain depth, which depends on the active acceptor concentration. This happens at a constant temperature and without altering the sample. A reverse voltage results in a downward band bending with respect to the Fermi level, and with increasing voltage the acceptors will be more and more populated with electrons and the free holes disappear from the surface region. Only a small forward voltage can be applied to the diode since the current increases strongly as soon as the built in voltage, produced by the Ti film, is compensated. This flat band condition corresponds to the original bulk situation.

For the experiment shown in Fig. 14 a Si sample was used with a low homogeneous concentration (1.3×10^{16} cm^{-3}) of stable In which was additionally implanted with ^{111}In at 60 keV and a dose of about 2×10^{12} cm^{-2}, corresponding to a peak concentration of 2×10^{17} cm^{-3} in a depth of 370 Å. Subsequently the sample was annealed and loaded with H in H_2O (358 K) for 21 h. At 300 K the Fourier spectrum [Fig. 14(a), top] shows a large fraction $f_{1/-}$ of $\nu_{Q1/-}$, in agreement with Fig. 5(a). After evaporation of the Ti film the concentration of free holes is reduced by applying a reverse bias that strongly enhances f_2 of ν_{Q2} at the expense of $f_{1/-}$ [see Fig. 14(a), bottom panel] as expected from the model discussed before. Application of a small forward bias of -1 V almost

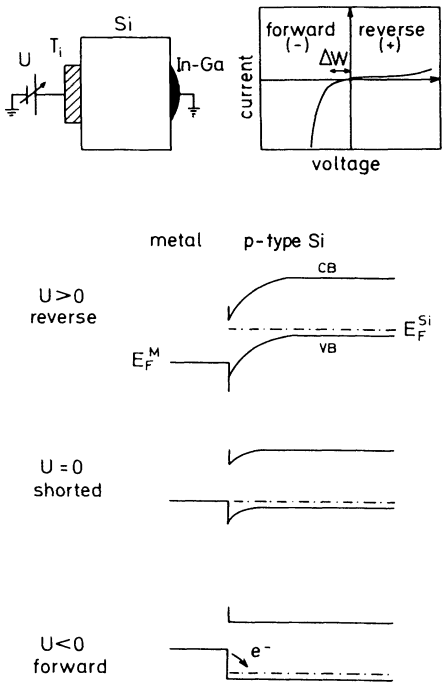

FIG. 13. Cross section of a Ti Schottky diode on p-type Si (top left). The asymmetric current-voltage characteristic is shifted with respect to zero bias by the difference of work functions ΔW between Ti and p-type Si (top right). Schematic band diagrams for different applied bias U (bottom).

restores the situation without film. The diode current and the fractions $f_{1/-}$ and f_2 extracted from the PAC measurements are plotted in Fig. 14(b) as a function of the applied voltage; these results are completely reversible. During the repopulation between $\nu_{Q1/-}$ and ν_{Q2} the sum of $f_{1/-}$ and f_2 remains constant, in agreement with the interpretation of Fig. 5(a).

In order to populate also $\nu_{Q1/0}$, Si samples with a B concentration exceeding the local ^{111}In concentration have to be used. Unavoidably the quality of the Schottky diodes suffers for acceptor concentrations above 10^{17} cm^{-3}. Therefore only small reverse voltages can be applied and the effects are smaller than in the experiment described above. In Fig. 15 the result of a sample with a homogeneous B concentration of 5×10^{18} cm^{-3}, partly passivated in H_2O, is shown. Again the ^{111}In atoms were implanted with 60 keV in order to position them closer to the surface, because the space-charge region only extends to several hundred angstroms in depth for this high dopant concentration. At 300 K the diode quality allowed the application of a reverse bias of +1 V and Fig. 15 shows that a growth of $f_{1/-}$ at the expense of $f_{1/0}$ was achieved by moving the Fermi level towards mid gap. In Fig. 5 this variation corresponds to a path parallel to the B concentration axis at 300 K where a transmutation of $\nu_{Q1/0}$ into $\nu_{Q1/-}$ is effected by the increasing Fermi level. Figure 16 shows the same experiment performed at 78 K where now a growth of f_2 at the expense of $f_{1/0}$ is observed for a maximum reverse bias of +2.4

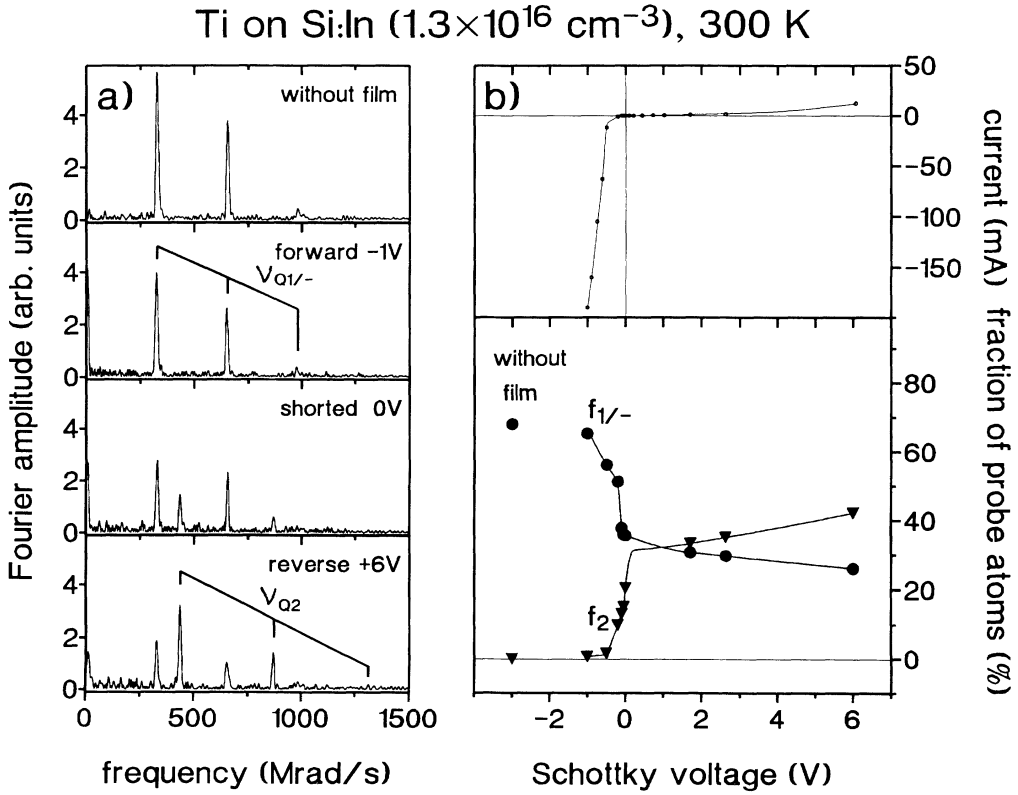

FIG. 14. (a) Fourier spectra of ^{111}In/Cd-H pairs in low-In-doped Schottky diode [Ti/(p-type Si)] at 300 K for different bias U and before evaporation of the Ti film. (b) Diode current (top) and repopulation between the fractions $f_{1/-}$ and f_2 (bottom) measured at 300 K as a function of the applied bias U.

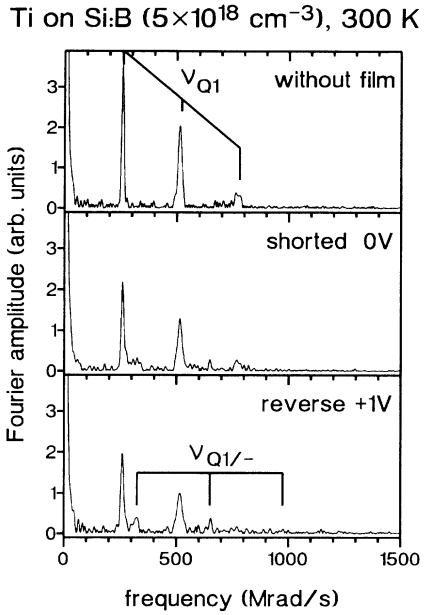

FIG. 15. Fourier spectra of ^{111}In/Cd-H pairs in a high-B doped (5×10^{18} cm^{-3}) Schottky diode at 300 K for different bias U and without Ti film.

V, as expected from Fig. 5(a) in which $\nu_{Q1/-}$ is replaced by ν_{Q2} at low temperatures because of the lower concentration of free holes.

These results confirm the interpretation given in Sec. IV that the population of the different states of Cd-H pairs is determined by the position of the Fermi level and the hole concentration and that, vice versa, the PAC signals allow to draw conclusions on the electronic state of the sample. Additionally the possibility of performing PAC experiments in the space-charge region of a Schottky diode was demonstrated. This is the prerequisite for a combination of the microscopically sensitive PAC with capacitance techniques like *C-V* profiling or DLTS, which would be helpful for the investigation of complexes with regard to their chemical identity and their electrical properties.

VI. SUMMARY

Semiconductor specific aspects for the application of PAC to defect studies were discussed using the example

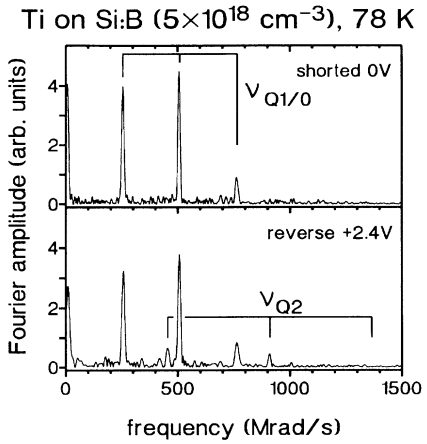

FIG. 16. Fourier spectra of the diode in Fig. 15 for different applied bias, but now at 78 K.

of ^{111}In-H pairs in Si. If a probe atom with a chemical transmutation like ^{111}In to ^{111}Cd is used, the measured structural properties are that of the residual complex (Cd-H) and not necessarily those of the originally formed one (In-H). However, the strengths of the PAC technique in identification, recognition, and study of formation and dissolution conditions of complexes are not weakened by this effect. In semiconductors the formed probe-atom–defect complex can possess different electronic states distinguished by different EFG's whose populations depend on the electronic conditions of the sample. This effect enhances the uniqueness of the PAC characteristic pattern of a complex and allows us to get additional information on the sample conditions directly from the PAC measurement. For In-H pairs in Si all data can be interpreted within a consistent picture, which was confirmed by experiments in Schottky diodes. In these experiments a change of the structure and the charge state of the complexes could be achieved by the applied bias and observed in the PAC measurements.

ACKNOWLEDGMENTS

This work has been financially supported by the Deutsche Forschungsgemeinschaft (SFB 306) and the Bundesminister für Forschung und Technologie.

[1]F. Pleiter and C. Hohenemser, Phys. Rev. B **25**, 106 (1982).
[2]E. Recknagel, G. Schatz, and Th. Wichert, in *Hyperfine Interactions of Radioactive Nuclei,* edited by J. Christiansen, Topics in Current Physics Vol. 31 (Springer, Berlin, 1983), p. 133.
[3]Th. Wichert, H. Skudlik, M. Deicher, G. Grübel, R. Keller, E. Recknagel, and L. Song, Phys. Rev. Lett. **59**, 2087 (1987).
[4]A. Baurichter, S. Deubler, D. Forkel, M. Gebhard, H. Wolf, and W. Witthuhn, Mater. Sci. Eng. B **4**, 281 (1989).
[5]Th. Wichert, M. Deicher, G. Grübel, R. Keller, N. Schulz, and H. Skudlik, Appl. Phys. A **48**, 59 (1989).
[6]R. Keller, M. Deicher, W. Pfeiffer, H. Skudlik, D. Steiner, and Th. Wichert, Phys. Rev. Lett. **65**, 2023 (1990).
[7]U. Reislöhner and W. Witthuhn, in *Proceedings of the Fourth International Conference on Shallow Impurities in Semiconductors,* Mater. Sci. Forum **65/66**, edited by G. Davies (Trans Tech, Aedermannsdorf, Switzerland, 1991), p. 281.
[8]A. Baurichter, M. Deicher, S. Deubler, D. Forkel, H. Plank, H. Wolf, and W. Witthuhn, Appl. Phys. Lett. **55**, 2301 (1989).
[9]W. Pfeiffer, M. Deicher, R. Keller, R. Magerle, E. Recknagel, H. Skudnik, Th. Wichert, H. Wolf, D. Forkel, N. Moriya, and R. Kalish, Appl. Phys. Lett. **58**, 1751 (1991).
[10]R. Magerle, M. Deicher, U. Desnica, R. Keller, W. Pfeiffer, F. Pleiter, H. Skudlik, and Th. Wichert, Appl. Surf. Sci. **50**, 159 (1991).

[11]R. Vianden, Hyperfine Interact. **61**, 1315 (1990).
[12]M. Deicher, G. Grübel, R. Keller, E. Recknagel, N. Schulz, H. Skudlik, and Th. Wichert, in *Proceedings of the 15th International Conference on Defects in Semiconductors,* Mater. Sci. Forum **38-41**, edited by G. Ferenczi (Trans Tech, Aedermannsdorf, Switzerland).
[13]H. Skudlik, M. Deicher, R. Keller, W. Pfeiffer, D. Steiner, and Th. Wichert, in *Defect Control in Semiconductors,* edited by K. Sumino (North-Holland, Amsterdam, 1990), p. 413.
[14]H. Skudlik, M. Deicher, R. Keller, R. Magerle, W. Pfeiffer, P. Pross, E. Recknagel, and Th. Wichert, following paper, Phys. Rev. B **46**, 2172 (1992).
[15]H. Frauenfelder and R. M. Steffen, in *Alpha-, Beta-, and Gamma-Ray Spectroscopy,* K. Siegbahn (North-Holland, Amsterdam, 1968), Vol. II, p. 997.
[16]H. H. Rinneberg, At. Energy Rev. **17**, 477 (1979).
[17]N. Achtziger, in *Submicroscopic Investigation of Defects in Semiconductors,* edited by G. Langouche (Elsevier, Amsterdam, in press).
[18]G. J. Kemerink and F. Pleiter, Phys. Lett. A **121**, 367 (1987).
[19]S. K. Estreicher, L. Throckmorton, and D. S. Marynick, Phys. Rev. B **39**, 13 241 (1989).
[20]P. J. H. Denteneer, C. G. Van de Walle, and S. T. Pantelides, Phys. Rev. B **39**, 10 809 (1989).
[21]D. Forkel, W. Engel, M. Iwatschenko-Borho, R. Keitel, and W. Witthuhn, Hyperfine Interact. **15/16**, 821 (1983).
[22]M. Gebhard, N. Achtziger, A. Baurichter, D. Forkel, B. Vogt, and W. Witthuhn, Physica B **170**, 320 (1991).
[23]H. Skudlik, M. Deicher, R. Keller, R. Magerle, W. Pfeiffer, and Th. Wichert (unpublished).